Author(s): Puttreddy, Rakesh; Topic, Filip; Valkonen, Arto; Rissanen, Kari

Title: Halogen-Bonded Co-Crystals of Aromatic N-oxides : Polydentate Acceptors for Halogen and Hydrogen Bonds

Year: 2017

Version:

Please cite the original version:

Puttreddy, R., Topic, F., Valkonen, A., & Rissanen, K. (2017). Halogen-Bonded Co-Crystals of Aromatic N-oxides : Polydentate Acceptors for Halogen and Hydrogen Bonds. Crystals, 7(7), Article 214. https://doi.org/10.3390/cryst7070214

crystals

MDPI

Article

Halogen-Bonded Co-Crystals of Aromatic *N*-oxides: Polydentate Acceptors for Halogen and Hydrogen Bonds

Rakesh Puttreddy *, Filip Topić, Arto Valkonen and Kari Rissanen *

Department of Chemistry, University of Jyvaskyla, P.O. Box 35, FI-40014 Jyvaskyla, Finland; filip.f.topic@jyu.fi (F.T.); arto.m.valkonen@jyu.fi (A.V.)

* Correspondence: rakesh.r.puttreddy@jyu.fi (R.P.); kari.t.rissanen@jyu.fi (K.R.); Tel.: +35-850-562-3721 (R.P. & K.R.)

Academic Editors: Peter Politzer and Jane S. Murray

Received: 7 June 2017; Accepted: 7 July 2017; Published: 11 July 2017

Abstract: Seventeen new halogen-bonded co-crystals characterized by single crystal X-ray analysis are presented from 8 × 4 combinations using methyl-substituted pyridine *N*-oxides and 1,ω-diiodoperfluoroalkanes. The N−O group in six of 17 co-crystals is monodentate and 11 have μ-*O,O* bidentate halogen bond acceptor modes. Remarkably, the N−O group in co-crystals of 3-methyl-, 4-methyl- and 3,4-dimethylpyridine*N*-oxides with octafluoro-1,4-diiodobutane acted as a μ-*O,O,O,O* halogen and hydrogen bond acceptor, while acting as a μ-*O,O,O* acceptor in the co-crystal of 2,5-dimethylpyridine*N*-oxide and tetrafluoro-1,2-diiodoethane. The C−H···O−N hydrogen bonds demonstrated the polydentate cooperativity of the N−O group as a mixed halogen-hydrogen bond acceptor. The co-crystal of 2,4,6-trimethylpyridine*N*-oxide and dodecafluoro-1,6-diiodohexane exhibited C−I···O^-−N^+ halogen bonds with R_{XB} value 0.76, the shortest of its kind compared to previously reported structures. The R_{XB} values between 0.76 and 0.83 suggested that the C−I···O^-−N^+ halogen bonds are moderately strong compared to our previously studied N^-−I^+···O^-−N^+ system, with R_{XB} in the order 0.66.

Keywords: halogen bond; hydrogen bond; aromatic *N*-oxides; perfluoroalkyl; diiodoperfluoroalkanes; polydentate; N−O group; cooperativity; C−H···O interactions

1. Introduction

The halogen bond (XB), analogous to the hydrogen bond (HB), has been defined [1] as a net attractive interaction between an electrophilic region of a halogen atom bound to a molecular entity and a nucleophilic site in another moiety, e.g., a nitrogen, oxygen or sulphur atom [2]. This region of positive electrostatic potential, called the "sigma hole" [3,4], is characteristic for halogen atoms attached to an organic backbone, with its magnitude generally decreasing in the order I > Br > Cl > F. Despite similar geometrical features between HB and XB, the halogen bond is still not as well-explored compared to the ubiquitous HB [5–9]. Halogen bonds are frequently studied using nitrogen compounds, which typically display monovalent N···X (X = I, Br) interactions and are well understood as crystal engineering tools for self-assembly processes. Their precedence from discrete structures to increased dimensionality through the controlled reactivity of substrates is well-reported [10–13]. In a solid-state XB complex, R−X···B−Z, where X is the donor and B is the acceptor atom, the ratio of the short distance between X and B atoms ($d_{X\text{-}B}$) to sum of the Van der Waals radii of X and B atoms (d_{vdW}) is defined as the normalized strength parameter, $R_{XB} = d_{X\text{-}B}/d_{vdW}$ [1]. Knowledge of R_{XB} values provides an opportunity to roughly estimate the strengths of XB complexes. For example, the X···N distances in bis(pyridine)iodonium(I) tetrafluoroborate constitute an R_{XB} value

of 0.65, and such compounds are classified as halogen bonds of covalent nature [14]. Carefully designed nitrogen compounds are successfully utilized as molecular building blocks engaging in $(N-X-N)^+X^-$ XBs to construct supramolecular structures resembling metal coordination frameworks [15]. However, weaker C−I···N XBs with typical R_{XB} values ranging from 0.75 to 0.90 are still of considerable importance for applications in materials chemistry, e.g., for triggering liquid crystallinity and gelation behaviour [16–18].

Aromatic *N*-oxides have been long known in heterocyclic chemistry for functionalized pyridines syntheses [19–25]. Besides being valuable synthetic intermediates, the dipolar neutral N^+-O^- group exhibits a push-pull property towards aromatic rings, enabling it to undergo both electrophilic and nucleophilic substitution reactions, categorizing these compounds as promising building blocks in supramolecular chemistry [26,27]. Electron-donating and electron-withdrawing substituents on aromatic ring invoke different hybridization states on oxygen in the N−O group [28,29], allowing for tuning of its complexation behaviour towards metals [30,31].

Strategic exploitation of XB acceptor properties for heteroatoms, such as oxygen, remains very much unknown in the literature. A Cambridge Structural Database (CSD) search for pyridine *N*-oxides functioning as XB acceptors revealed only a handful of structures (see supporting information for more details), while their systematic investigations remain especially scarce [32–34]. Previously, monodentate strong $N^--I^+\cdots O^--N^+$ XBs (R_{XB} as low as 0.66) of coordinative nature between pyridine *N*-oxides and N-haloimides were studied both in solution and in the solid-state [35]. Here, we aimed to investigate $C-I\cdots O^--N^+$ XBs using 1,ω-diiodoperfluoroalkanes (DI2–DI8) and methyl-substituted aromatic *N*-oxides (1–8), as shown in Figure 1. Haloperfluoroalkanes are robust XB donors, and their ability to steer the supramolecular assembly by XBs and F···F interactions is well described [36]. However, the volatile nature of these compounds often results in oily or waxy substances, which are difficult to characterize using single crystal X-ray diffraction [18,37]. Despite their reluctance to crystallize, our attempts from 8 × 4 (acceptor × donor) combinations resulted in 17 crystal structures, providing an impressive crystallization success rate to analyze and understand the interactions at play in their solid-state structures.

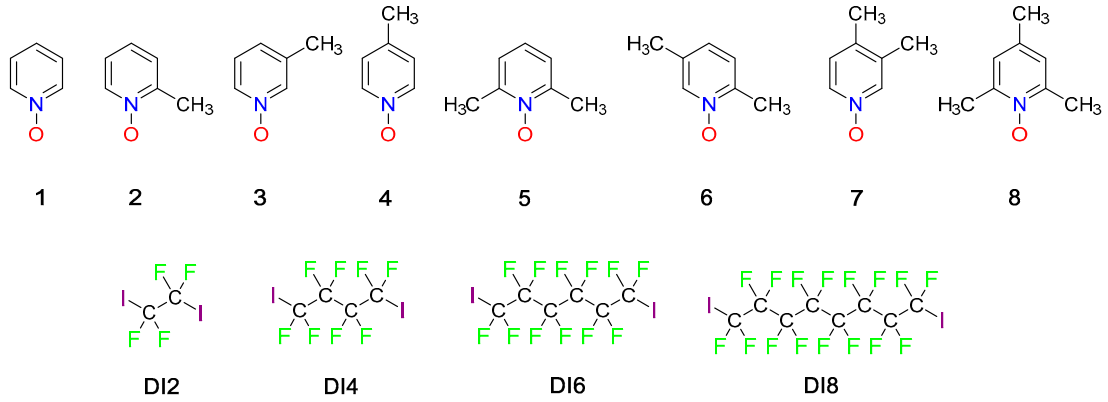

Figure 1. The chemical structures of acceptors (top) and donors (below) in the current study: pyridine *N*-oxide (1), 2-methylpyridine *N*-oxide (2), 3-methylpyridine *N*-oxide (3), 4-methylpyridine *N*-oxide (4), 2,6-dimethylpyridine *N*-oxide (5), 2,5-dimethylpyridine *N*-oxide (6), 3,4-dimethylpyridine *N*-oxide (7), 2,4,6-trimethylpyridine *N*-oxide (8), tetrafluoro-1,2-diiodoethane (DI2), octafluoro-1,4-diiodobutane (DI4), dodecafluoro-1,6-diiodohexane (DI6) and hexadecafluoro-1,8-diiodooctane (DI8).

2. Results and Discussion

The methods used to obtain the single crystals suitable for X-ray analysis are shown in Table S1. Co-crystals 1•DI6, 1•DI8, 2•DI4, 3•DI4, 3•DI8, 4•DI4_I, 4•DI4_II, 5•DI2, 5•DI6, 7•DI4 and 7•DI6 all form infinite 1-D polymers, and 4•DI4_I and 4•DI4_II are polymorphs. The co-crystals were grouped and discussed based on structural similarities observed in the crystal packing. Halogen

bonds between N−O and C−I groups were explored as the driving force propagating 1-D polymers with alternate acceptors and donors. The XB interaction bond parameters are shown in Table 1. In 1●DI6, 1●DI8 and 3●DI8, the aromatic rings and donors were essentially coplanar, in contrast to the orthogonal alignment typically observed in coordination compounds [30,31]. The N−O groups were μ-*O,O* bidentate, bridging the donors to form remarkably similar 1-D polymeric chains, as shown in Figure 2. Further analysis of the crystal packing revealed the donor-acceptor parallel arrangement to be a result of F···F aggregation [38–42] between perfluorinated donor chains, which, though weaker than C−I···O^-−N^+ XBs, play a crucial role to yield a robust 3-D crystal structure.

Table 1. Bond parameters for co-crystals 1●DI6–8●DI6.

S.No	Code	Monodentate		μ-*O,O*	
		ca. d(I···O−N)/Å *	∠(C−I···O)/°	*ca. d*(I···O−N)/Å *	∠(C−I···O)/°
1	1●DI6	2.834 [0.81]	177.1	**	**
2	1●DI8	2.833 [0.81]	177.7	**	**
3	2●DI4	2.747 [0.79]	174.2	2.861 [0.82]	178.9
4	3●DI4	2.840 [0.81]	172.1	2.875 [0.82]	168.8
5	3●DI8	2.809 [0.80]	174.8	2.817 [0.81]	174.7
6	4●DI4_I	2.808 [0.80] ***	172.3 ***	2.813 [0.80] ***	174.1 ***
7	4●DI4_II	2.766 [0.79]	177.5 ***	**	**
8	5●DI2	2.743 [0.78]	161.2 ***	**	**
9	5●DI4	2.669 [0.76]	171.3 ***	–	–
10	5●DI6	2.733 [0.78]	175.5	2.774 [0.80]	169.0
		2.764 [0.79]	174.9	2.813 [0.804]	170.3
11	6●DI2	2.714 [0.78]	171.9	–	–
12	7●DI2	2.703 [0.77]	174.6	–	–
13	7●DI4	2.835 [0.81]	167.5 ***	2.906 [0.83]	170.0 ***
14	7●DI6	2.825 [0.81]	167.9 ***	2.827 [0.81]	178.2 ***
15	7●DI8	2.715 [0.78]	176.5	–	–
16	8●DI2	2.702 [0.78]	166.4	–	–
		2.775 [0.79]	170.8	–	–
17	8●DI6	2.649 [0.76]	174.3	–	–
		2.682 [0.77]	176.1	–	–

* Respective R_{XB} values are reported in parentheses [1]. ** The other halogen bond is symmetrically equivalent. *** Major disorder component.

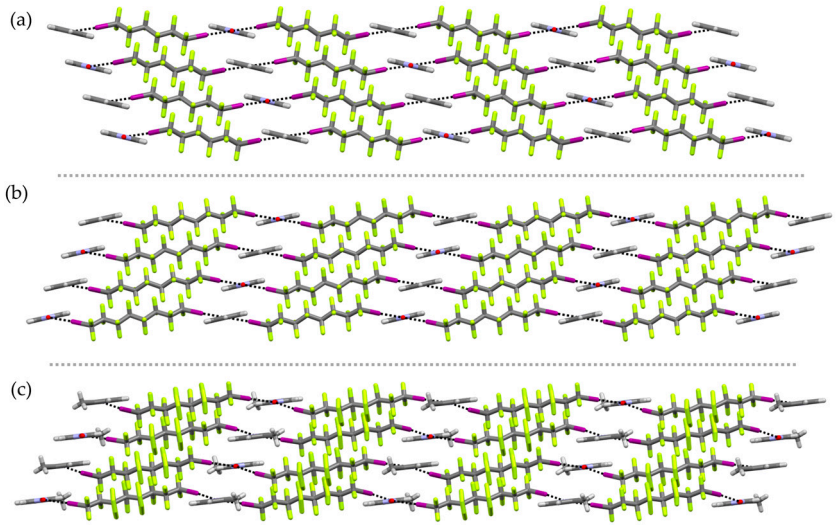

Figure 2. Section of the crystal packing showing structural similarity between 1-D parallel stacks in 1●DI6 (**a**), 1●DI8 (**b**) and 3●DI8 (**c**).

The strength of the C−H···O interaction is approximately one-third of conventional HBs [43–49] that operate between donors such as −N−H/−O−H and weak bases, and these interactions significantly increase the lattice energy of the co-crystals [50]. The C−H···O contacts are attractive, and are rather site acidity-dependent. For example, the C2-proton acidity in pyridine *N*-oxides for *ortho*-C−H functionalization in organic synthesis [19–25], and in crystal engineering for C−H···O−N interactions is well studied [51–54]. However, to the best of our knowledge, the combination of C−H···O−N and C−I···O−N interactions through the N−O group, giving rise to supramolecular assemblies, has not been extensively studied. Co-crystals 3•DI4, 4•DI4_I, 7•DI4, and 7•DI6 all formed 1-D polymers driven majorly by C−I···O−N interactions; however, C−H···O interactions orthogonal to XB chains were interpreted as an essential element of the co-crystal structure. For example, in 3•DI4, the N−O group bridged donors at I···O distances of *ca.* 2.840 Å (R_{XB} = 0.81) and *ca.* 2.875 Å (R_{XB} = 0.82) with I···O···I angles of *ca.* 139.6°, leading to 1-D polymers. Orthogonal to μ-*O,O* XB mode, C−H···O interactions operated between N−O groups and C2-/C6-protons in the ab-plane to form 2-D sheets (Figure 3a). The perfluorinated chains and aromatic rings from adjacent 1-D polymers aggregated through F···F and C−H···O interactions, and induced segregation of donors and acceptors in the crystal structure. Similar *ortho*-C−H···O interactions between *N*-oxide molecules, and donor-acceptor segregated crystal packing motifs were observed in 4•DI4_I, 7•DI4 and 7•DI6 (Figure 3b–d).

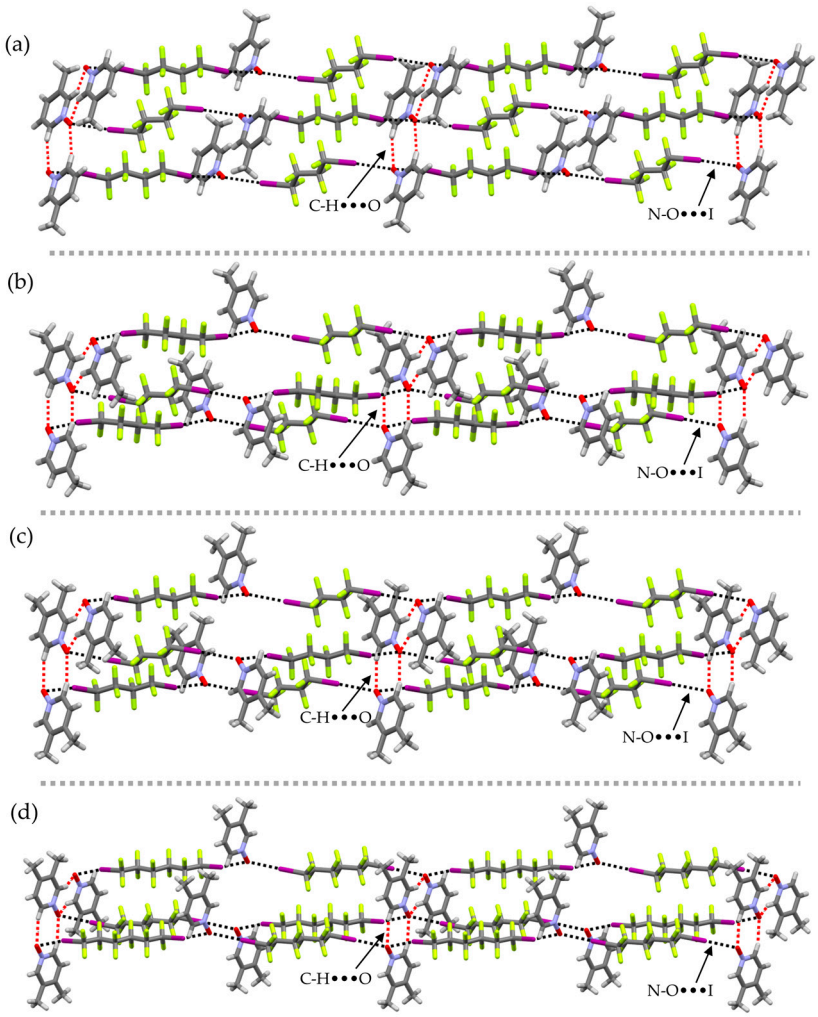

Figure 3. 1-D Halogen bond polymers stitched by adjacent *ortho*-C−H···O interactions in, 3•DI4 (**a**), 4•DI4_I (**b**), 7•DI4 (**c**) and 7•DI6 (**d**) shown in capped stick models. Black and red broken lines are respectively XB and HB interactions.

Structures of co-crystals 2●DI4, 4●DI4_II, 5●DI2 and 5●DI6 showed 1-D undulating patterns driven by C−I···O−N interactions, as depicted in Figure 4. The I···O···I angles and the centroid-to-centroid distances between aromatic rings occupying the crest and trough sites were directly related. For example, the 2●DI4 (145.2°) and 4●DI4_II (112.2°) manifested a shallow wave appearance, with centroid-to-centroid aromatic distances of 23.2 Å and 19.2 Å, respectively. These I···O···I angles were greater than in 5●DI2 (103.6°) and 5●DI6 (107.8°), which both exhibited sharp interwoven patterns with the respective centroid-to-centroid aromatic distances of 16.9 Å and 17.2 Å. In 5●DI2 and 5●DI6, the aromatic rings were orthogonal to μ-*O,O* XB mode, favouring closer interdigitation between 1-D chains stabilized by C−H···F interactions. Moreover, the 1-D XB chains were cross-aligned in 2●DI4 (Figure 4b), different from parallel stack observed in 4●DI4_II, 5●DI2 and 5●DI6 (Figure 4f). In these structures, the aromatic rings did not participate in any π···π interactions, and the structures were sustained by several weak F···F, C−H···O and C−H···F interactions.

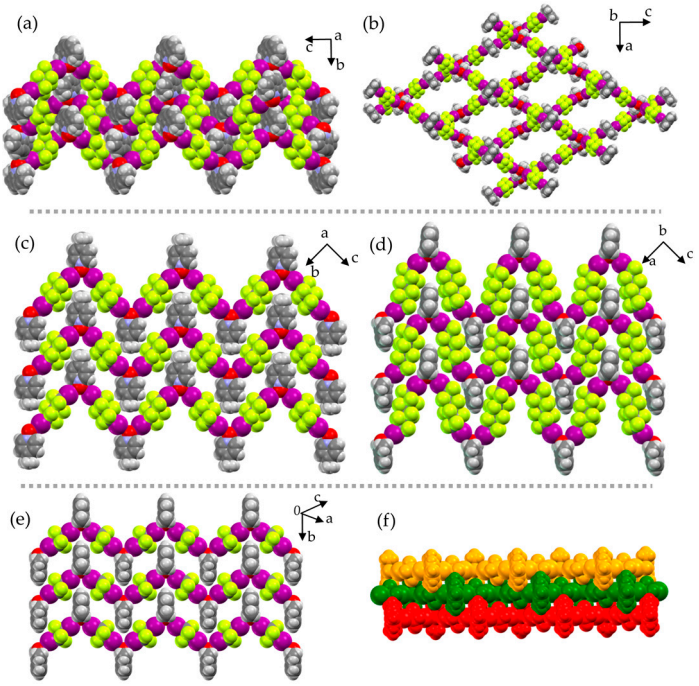

Figure 4. Interwoven by C−H···F interactions, the 1-D undulated XB polymeric chains in 2●DI4 (**a**), 4●DI4_II (**c**), 5●DI6 (**d**) and 5●DI2 (**e**). Section of 3-D crystal packing in 2●DI4 (**b**) showing cross stack of 1-D polymers, and common parallel 1-D stack motifs observed in 4●DI4_II, 5●DI6 and 5●DI2 (**f**).

The N−O groups in co-crystals 7●DI2 and 7●DI8 act as monodentate XB acceptors with I···O distances *ca*. 2.703 Å (R_{XB} = 0.77) and *ca*. 2.715 Å (R_{XB} = 0.78). Contrary to above examples, the C−H···O interactions became more pronounced in 7●DI2 and 7●DI8, breaking the XB continuity in 1-D chains, and inducing alternate XB and cyclic C−H···O interactions as seen in Figure 5. The molecules of 7 could be seen as forming fully planar dimers, which were further connected by XB respectively with DI2 or DI8. In 7●DI2, the offset stacking of the acceptor dimers prevented the formation of F···F interactions by DI2 (Figure 5c). In 7●DI8, due to longer DI8 chains, the π···π stacking prevented only a half of the perfluorooctane chain from establishing F···F interactions (Figure 5d), with the packing in co-crystals 7●DI2 and 7●DI8 being otherwise quite similar.

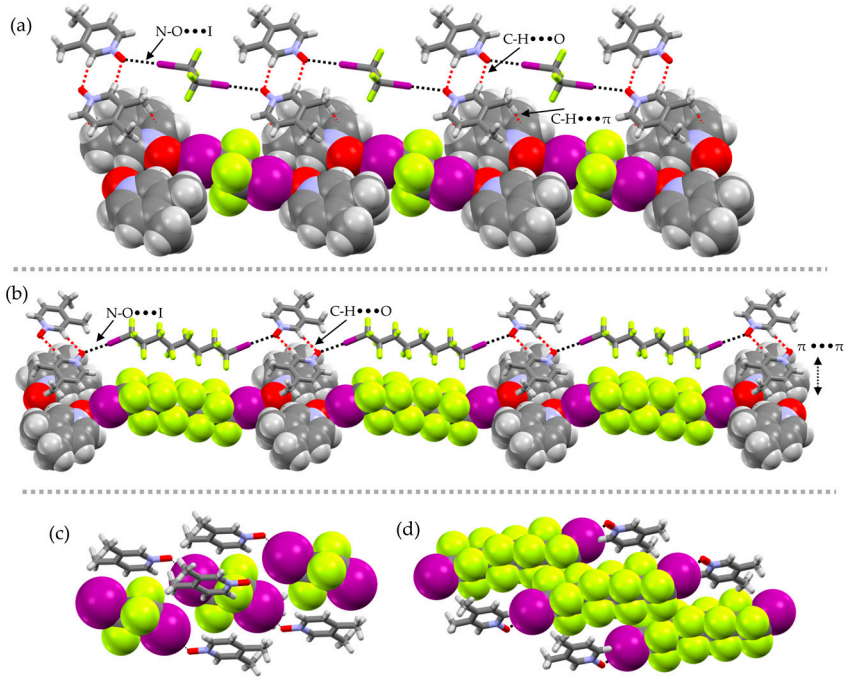

Figure 5. 1-D Chains propagated by alternating XB and C−H···O interactions in 7•DI2 (**a**) and 7•DI8 (**b**). Section of crystal packing displaying isolated DI2 in 7•DI2 (**c**), and partially F···F stabilized DI8 in 7•DI8 (**d**). Black and red broken lines are respectively XB and HB interactions.

The 6•DI2 exhibited a 1:2 donor-acceptor stoichiometry, crystallizing in the monoclinic space group $P2_1/n$, with the donor molecule DI2 lying on an inversion centre. A XB with I···O distances of *ca*. 2.714 (R_{XB} = 0.78) and two C−H···O−N interactions at N−O group suggested sp^3 hybridization of the oxygen. The C−H···O interactions played a significant role in the crystal packing. Analysis of the interlayer packing revealed the formation of a 1-D zig-zag HB tape along the b-axis (Figure 6a) through C−H···O interactions between the N−O group and the C2-methyl and C6-hydrogens. The 1-D tapes were connected by DI2 (Figure 6b) to give 2-D sheets which further stacked along the third dimension, with centroid-to-centroid aromatic distances of *ca*. 3.84 Å.

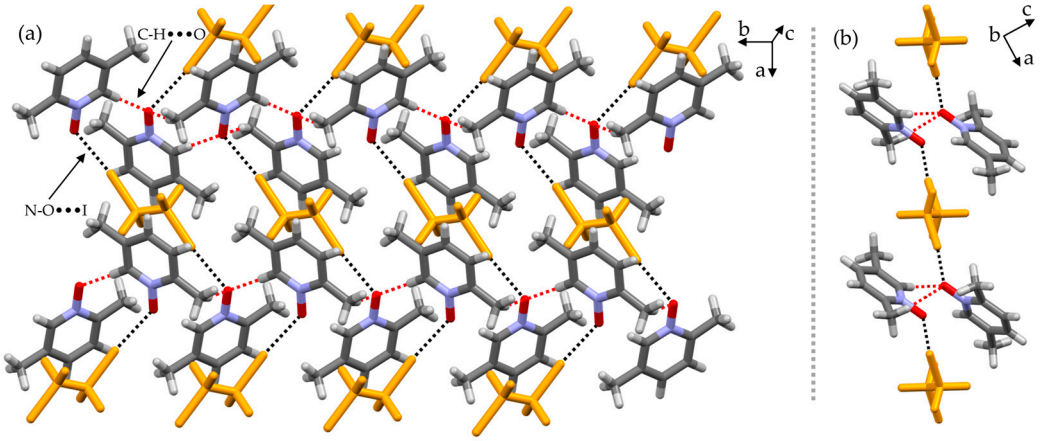

Figure 6. The 1-D Hydrogen bond tapes bridged by DI2 donors (**a**), and a view along the b-axis showing connecting modes of DI2 (**b**). Color representation: Gold capped sticks are DI2 donors, black and red broken lines are respectively XB and HB interactions.

Co-crystals 5•DI4, 8•DI2 and 8•DI6 also formed 2:1 acceptor-donor discrete structures (Figure 7a–c), with monodentate XB acceptor modes for N−O groups. In 5•DI4, the 1:2 discrete units propagated along the *b*-axis by C−H···O interactions between N−O and methyl groups. Further, the 1-D motifs (Figure 7d) extended three dimensionally through C−H···F and π···π interactions. Co-crystal 8•DI2 had an interesting 1-D ladder structure (Figure 7f), with *N*-oxides forming 1-D tapes through C−H···O interactions as the side rails (Figure 7g) connected by halogen bonds via DI2. These 1-D ladders further packed through stacking of the aromatic rings as depicted schematically in Figure 7h. On the other hand, 8•DI6 with its 3:1 acceptor-donor generated a more complex structure, extended by π···π interactions between 2:1 discrete units and the additional, "passive" molecule of *N*-oxide 8, not involved in XB, as depicted in Figure 7e. While the "passive" molecule of 8, situated near an inversion centre, was disordered over two components with 50:50 occupancies, the *anti-gauche* conformation of DI6 was not compatible with the presence of an inversion centre in the middle of the C3-C4 bond of the donor.

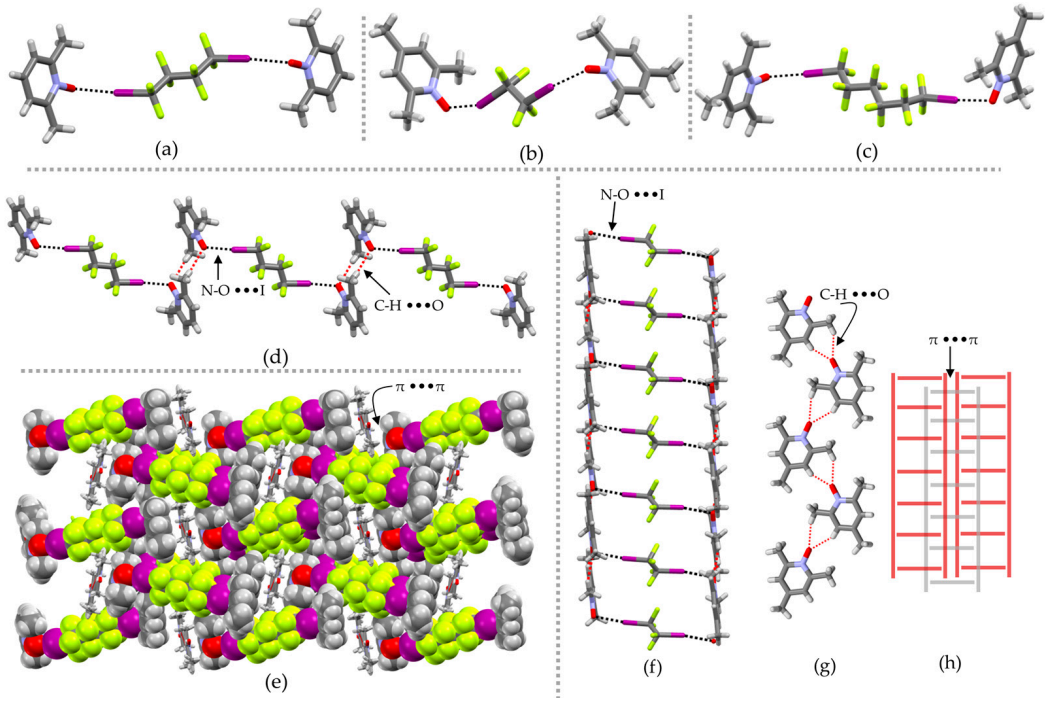

Figure 7. 2:1 Acceptor-donor discrete structures in 5•DI4 (**a**) 8•DI2 (**b**) and 8•DI6 (**c**). The C−H···O interactions connect the 2:1 units in 5•DI4 (**d**). Complex crystal packing in 8•DI6 displaying π···π interactions stabilized 2:1 units (**e**); 1-D Ladder motif in 8•DI2 (**f**), and the 1-D HB tapes formed by 8 (**g**). Cartoon of 1-D ladders illustrating the π-π stacking in 8•DI2 (**h**). Black and red broken lines are respectively XB and HB interactions.

3. Conclusions

Halogen bonding between pyridine *N*-oxides and 1,ω-diiodoperfluoroalkanes was found to be a reliable tool for crystal engineering, as witnessed by the successful structural characterization of 17 co-crystals reported here. The *N*-oxide functionality was able to act as either a monodentate (6/17 co-crystals) or μ-*O,O* bidentate (11/17 co-crystals) halogen bond acceptor. Monodentate C−I···O^-−N^+ halogen bonds were stronger than bidentate C−I···O^-−N^+ halogen bonds. Based on the observed R_{XB} values, ranging from 0.76 to 0.83, C−I···O^-−N^+ halogen bonds can be classified as moderately strong compared to e.g. very strong monodentate N^-−I^+···O^-−N^+ type halogen bonds, previously studied by us, which display R_{XB} values as low as 0.66. In addition to that, an important role of weak interactions, such as weak C−H···O hydrogen bonds and aromatic ring stacking, has

been established. In particular, the *N*-oxide oxygen atom was shown to simultaneously engage in both the hydrogen and halogen bonding as a mixed acceptor. However, the C−H···O hydrogen bonds were fairly weak, as witnessed by the observation of two polymorphs of 4•DI4, where only one of the two exhibited C−H···O hydrogen bonds. The ability of *N*-oxide oxygen to act as a μ_2- (one XB and one HB), μ_3- (one XB and two HB) and μ_4-acceptor (two XB and two HB) is a complex process. For example, the pronounced C−H···O hydrogen bonds between *N*-oxide oxygen and C2- acidic protons can be a result of F···F interaction [38–42] between adjacent perfluorinated donor chains, resulting in a stable crystal lattice.

4. Materials and Instrumentation

All solvents used for crystal growth were of reagent grade, and used as received. Pyridine *N*-oxide (1), 2-methylpyridine *N*-oxide (2), 3-methylpyridine *N*-oxide (3), 4-methylpyridine *N*-oxide (4), 2,6-dimethylpyridine *N*-oxide (5) and hexadecafluoro-1,8-diiodooctane (DI8) were purchased from Sigma-Aldrich, while tetrafluoro-1,2-ethane (DI2), octafluoro-1,4-diiodobutane (DI4), and dodecafluoro-1,6-diiodohexane (DI6) were purchased from Apollo Scientific Chemicals Ltd. 2,5-Dimethylpyridine *N*-oxide (6), 3,4-dimethylpyridine *N*-oxide (7) and 2,4,6-trimethylpyridine *N*-oxide (8) were synthesized as previously reported [29].

Single crystal X-ray data for 1•DI6, 1•DI8, 2•DI4, 3•DI4, 4•DI4_I, 4•DI4_II, 5•DI4, 7•DI2, 7•DI4, 7•DI6 and 8•DI2 were measured on a Bruker-Nonius Kappa CCD diffractometer (Bruker AXS Inc, Wisconsin, USA) with an APEX-II CCD detector using graphite-monochromated Mo-Kα (λ = 0.71073 Å) radiation. The data for 3•DI8, 5•DI2, 5•DI6, 6•DI2, 7•DI8, and 8•DI6 were measured on an RigakuOxford single-source diffractometer (Rigaku Corporation, Tokyo, Japan) equipped with an Eos CCD detector using mirror-monochromated Mo-*K*α (λ = 0.71073 Å) radiation. The crystal data and experimental details for the data collections are given in Tables S2–S5. Data collection and reduction for Rigaku Oxford diffractometer were performed using the program *CrysAlisPro* [55], while for Bruker-Nonius Kappa CCD diffractometer using the program COLLECT [56] and HKL DENZO AND SCALEPACK [57]. A Gaussian face indexing-based absorption correction method [55] was used for 3•DI8, 5•DI2, 5•DI6 and 7•DI8, while the multi-scan absorption correction through CrysAlisPro [55] was used for **8**•DI6 and through SADABS [58] for 1•DI6, 1•DI8, 2•DI4, 3•DI4, 4•DI4_I, 4•DI4_II, 5•DI4, 6•DI2, 7•DI2, 7•DI4, 7•DI6 and 8•DI2. The structures were solved with direct methods (either SHELXS or SHELXT) [59] and refined by full-matrix least squares on F^2 using OLEX2 [60] and/or WinGX [61] which utilize the SHELXL-2016/6 module [59]. No attempt was made to locate the hydrogens from difference electron density Fourier maps, and appropriate constraints and restraints were used when necessary for disordered molecules.

Supplementary Materials: The following are available online at www.mdpi.com/2073-4352/7/7/214/s1, Table S1: Summary of crystallization experiments, Table S2: Crystal data and X-ray experimental details for 1•DI4–3•DI8, Table S3: Crystal data and X-ray experimental details for 4•DI4_I–5•DI6. Table S4: Crystal data and X-ray experimental details for 6•DI2–7•DI8. Table S5: Crystal data and X-ray experimental details for 8•DI2 and 8•DI6. Figure S1: Scatter plot of N-O···I angles vs. I···O distances in *N*-oxide oxygens functioning as halogen bond acceptors, as found in CCDC. Figure S2: Scatter plot of N−O···I angles vs. I···O distances as a comparison of our previous and current results of *N*-oxide oxygens functioning as halogen bond acceptors.

Acknowledgments: The authors kindly acknowledge the Academy of Finland (Project numbers RP: 298817, KR: 263256, 265328 and 292746) and the University of Jyväskylä for financial support.

Author Contributions: The synthesis of aromatic *N*-oxides and the project design presented in this work were performed by R.P. X-ray analysis and structural solution for eight structures was obtained by R.P., eight by F.T. and one by A.V. The manuscript was written by R.P. and assisted by F.T., and K.R. supervised the work.

Conflicts of Interest: The authors declare no conflict of interest.

References and Notes

1. Desiraju, R.G.; Ho, S.P.; Kloo, L.; Legon, C.A.; Marquardt, R.; Metrangolo, P.; Politzer, P.; Resnati, G.; Rissanen, K. Definition of the halogen bond (IUPAC Recommendations 2013). *Pure Appl. Chem.* **2013**, *85*, 1711–1713. [CrossRef]
2. *Halogen Bonding*, 2008th ed.; Metrangolo, P.; Resnati, G. (Eds.) Springer: Berlin, Germany, 2008; Volume 126.
3. Politzer, P.; Murray, J.S. Halogen bonding: An interim discussion. *ChemPhysChem* **2013**, *14*, 278–294. [CrossRef] [PubMed]
4. Politzer, P.; Murray, J.S.; Clark, T. Halogen bonding and other [sigma]-hole interactions: A perspective. *Phys. Chem. Chem. Phys.* **2013**, *15*, 11178–11189. [CrossRef] [PubMed]
5. Rissanen, K. Halogen bonded supramolecular complexes and networks. *CrystEngComm* **2008**, *10*, 1107–1113. [CrossRef]
6. Troff, R.W.; Mäkelä, T.; Topić, F.; Valkonen, A.; Raatikainen, K.; Rissanen, K. Alternative motifs for halogen bonding. *Eur. J. Org. Chem.* **2013**, *2013*, 1617–1637. [CrossRef]
7. Metrangolo, P.; Meyer, F.; Pilati, T.; Resnati, G.; Terraneo, G. Halogen bonding in supramolecular chemistry. *Angew. Chem. Int. Ed.* **2008**, *47*, 6114–6127. [CrossRef] [PubMed]
8. Priimagi, A.; Cavallo, G.; Metrangolo, P.; Resnati, G. The halogen bond in the design of functional supramolecular materials: Recent advances. *Acc. Chem. Res.* **2013**, *46*, 2686–2695. [CrossRef] [PubMed]
9. Voth, A.R.; Khuu, P.; Oishi, K.; Ho, P.S. Halogen bonds as orthogonal molecular interactions to hydrogen bonds. *Nat. Chem.* **2009**, *1*, 74–79. [CrossRef] [PubMed]
10. Bedin, M.; Karim, A.; Reitti, M.; Carlsson, A.-C.C.; Topić, F.; Cetina, M.; Pan, F.; Havel, V.; Al-Ameri, F.; Sindelar, V.; et al. Counterion influence on the $[N\text{-}I\text{-}N]^+$ halogen bond. *Chem. Sci.* **2015**, *6*, 3746–3756. [CrossRef]
11. Carlsson, A.-C.C.; Gräfenstein, J.; Budnjo, A.; Laurila, J.L.; Bergquist, J.; Karim, A.; Kleinmaier, R.; Brath, U.; Erdélyi, M. Symmetric halogen bonding is preferred in solution. *J. Am. Chem. Soc.* **2012**, *134*, 5706–5715. [CrossRef] [PubMed]
12. Carlsson, A.-C.C.; Veiga, A.; Erdélyi, M. Halogen bonding in solution. In *Halogen Bonding II SE-607*; Metrangolo, P., Resnati, G., Eds.; Springer: Berlin, Germany, 2015; Volume 359, pp. 49–76.
13. Rissanen, K.; Haukka, M. Halonium Ions as Halogen Bond Donors in the Solid State $[XL_2]Y$ Complexes. In *Halogen Bonding II SE-587*; Metrangolo, P., Resnati, G., Eds.; Springer: Berlin, Germany, 2015; Volume 359, pp. 77–90.
14. Barluenga, J.; González, J.M.; Campos, P.J.; Asensio, G. $I(Py)_2BF_4$, a new reagent in organic synthesis: General method for the 1,2-Iodofunctionalization of olefins. *Angew. Chem. Int. Ed.* **1985**, *24*, 319–320. [CrossRef]
15. Turunen, L.; Warzok, U.; Puttreddy, R.; Beyeh, N.K.; Schalley, C.A.; Rissanen, K. $[N\cdots I^+\cdots N]$ halogen-bonded dimeric capsules from tetrakis(3-pyridyl)ethylene cavitands. *Angew. Chem. Int. Ed.* **2016**, *55*, 14033–14036. [CrossRef] [PubMed]
16. Fourmigué, M. Halogen bonding: Recent advances. *Curr. Opin. Solid State Mater. Sci.* **2009**, *13*, 36–45. [CrossRef]
17. Nguyen, H.L.; Horton, P.N.; Hursthouse, M.B.; Legon, A.C.; Bruce, D.W. Halogen bonding: A new interaction for liquid crystal formation. *J. Am. Chem. Soc.* **2004**, *126*, 16–17. [CrossRef] [PubMed]
18. Metrangolo, P.; Prasang, C.; Resnati, G.; Liantonio, R.; Whitwood, A.C.; Bruce, D.W. Fluorinated liquid crystals formed by halogen bonding. *Chem. Commun.* **2006**, 3290–3292. [CrossRef] [PubMed]
19. Bull, J.A.; Mousseau, J.J.; Pelletier, G.; Charette, A.B. Synthesis of pyridine and dihydropyridine derivatives by regio- and stereoselective addition to N-activated pyridines. *Chem. Rev.* **2012**, *112*, 2642–2713. [CrossRef] [PubMed]
20. Xiao, B.; Liu, Z.-J.; Liu, L.; Fu, Y. Palladium-catalyzed C–H activation/cross-coupling of pyridine *N*-oxides with nonactivated secondary alkyl bromides. *J. Am. Chem. Soc.* **2013**, *135*, 616–619. [CrossRef] [PubMed]
21. Wu, J.; Cui, X.; Chen, L.; Jiang, G.; Wu, Y. Palladium-catalyzed alkenylation of quinoline-*N*-oxides via C−H activation under external-oxidant-free conditions. *J. Am. Chem. Soc.* **2009**, *131*, 13888–13889. [CrossRef] [PubMed]
22. Campeau, L.-C.; Schipper, D.J.; Fagnou, K. Site-selective sp^2 and benzylic sp^3 palladium-catalyzed direct arylation. *J. Am. Chem. Soc.* **2008**, *130*, 3266–3267. [CrossRef] [PubMed]

23. Campeau, L.-C.; Bertrand-Laperle, M.; Leclerc, J.-P.; Villemure, E.; Gorelsky, S.; Fagnou, K. C2, C5, and C4 azole *N*-oxide direct arylation including room-temperature reactions. *J. Am. Chem. Soc.* **2008**, *130*, 3276–3277. [CrossRef] [PubMed]
24. Pool, J.A.; Scott, B.L.; Kiplinger, J.L. A new mode of reactivity for pyridine *N*-oxide: C−H activation with uranium(IV) and thorium(IV) bis(alkyl) complexes. *J. Am. Chem. Soc.* **2005**, *127*, 1338–1339. [CrossRef] [PubMed]
25. Campeau, L.-C.; Rousseaux, S.; Fagnou, K. A solution to the 2-Pyridyl organometallic cross-coupling problem: Regioselective catalytic direct arylation of pyridine *N*-oxides. *J. Am. Chem. Soc.* **2005**, *127*, 18020–18021. [CrossRef] [PubMed]
26. Adriaenssens, L.; Ballester, P. Hydrogen bonded supramolecular capsules with functionalized interiors: The controlled orientation of included guests. *Chem. Soc. Rev.* **2013**, *42*, 3261–3277. [CrossRef] [PubMed]
27. Raynal, M.; Ballester, P.; Vidal-Ferran, A.; van Leeuwen, P.W. Supramolecular catalysis. Part 1: Non-covalent interactions as a tool for building and modifying homogeneous catalysts. *Chem. Soc. Rev.* **2014**, *43*, 1660–1733. [CrossRef] [PubMed]
28. Albini, A. *Heterocyclic N-oxides*; CRC Press: Boca Raton, FL, USA, 1991.
29. Katritzky, A.R.; Lagowski, J.M. *Chemistry of the Heterocyclic N-oxides*; Academic Press: Cambridge, MA, USA, 1971.
30. Puttreddy, R.; Steel, P.J. 4-Methoxypyridine *N*-oxide: An electron-rich ligand that can simultaneously bridge three silver atoms. *Inorg. Chem. Commun.* **2014**, *41*, 33–36. [CrossRef]
31. Puttreddy, R.; Steel, P.J. Pyridine *N*-oxide: A hyperdentate argentophile. *CrystEngComm* **2014**, *16*, 556–560. [CrossRef]
32. Pang, X.; Jin, W.J. Exploring the halogen bond specific solvent effects in halogenated solvent systems by ESR probe. *New J. Chem.* **2015**, *39*, 5477–5483. [CrossRef]
33. Aakeröy, C.B.; Wijethunga, T.K.; Desper, J. Constructing molecular polygons using halogen bonding and bifurcated *N*-oxides. *CrystEngComm* **2014**, *16*, 28–31. [CrossRef]
34. Messina, M.T.; Metrangolo, P.; Panzeri, W.; Pilati, T.; Resnati, G. Intermolecular recognition between hydrocarbon oxygen-donors and perfluorocarbon iodine-acceptors: The shortest O···I non-covalent bond. *Tetrahedron* **2001**, *57*, 8543–8550. [CrossRef]
35. Puttreddy, R.; Jurček, O.; Bhowmik, S.; Makela, T.; Rissanen, K. Very strong $^{-}$N-X$^{+}\cdots^{-}$O-N^{+} halogen bonds. *Chem. Commun.* **2016**, *11*, 2338–2341. [CrossRef] [PubMed]
36. Ho, P.S. Halogen Bonding I. *Top. Curr. Chem.* **2015**, *358*, 241–276. [PubMed]
37. Aakeröy, C.B.; Wijethunga, T.K.; Benton, J.; Desper, J. Stabilizing volatile liquid chemicals using co-crystallization. *Chem. Commun.* **2015**, *51*, 2425–2428. [CrossRef] [PubMed]
38. Omorodion, H.; Twamley, B.; Platts, J.A.; Baker, R.J. Further evidence on the importance of fluorous–fluorous interactions in supramolecular chemistry: A combined structural and computational study. *Cryst. Growth Des.* **2015**, *15*, 2835–2841. [CrossRef]
39. Baker, R.J.; Colavita, P.E.; Murphy, D.M.; Platts, J.A.; Wallis, J.D. Fluorine–fluorine interactions in the solid state: An experimental and theoretical study. *J. Phys. Chem. A* **2012**, *116*, 1435–1444. [CrossRef] [PubMed]
40. Reichenbacher, K.; Suss, H.I.; Hulliger, J. Fluorine in crystal engineering—"The little atom that could". *Chem. Soc. Rev.* **2005**, *34*, 22–30. [CrossRef] [PubMed]
41. O'Hagan, D. Understanding organofluorine chemistry. An introduction to the C–F bond. *Chem. Soc. Rev.* **2008**, *37*, 308–319. [CrossRef] [PubMed]
42. Berger, R.; Resnati, G.; Metrangolo, P.; Weber, E.; Hulliger, J. Organic fluorine compounds: A great opportunity for enhanced materials properties. *Chem. Soc. Rev.* **2011**, *40*, 3496–3508. [CrossRef] [PubMed]
43. Taylor, R. It Isn't, It Is: The C–H···X (X = O, N, F, Cl) interaction really is significant in crystal packing. *Cryst. Growth Des.* **2016**, *16*, 4165–4168. [CrossRef]
44. Dragelj, J.L.; Stanković, I.M.; Božinovski, D.M.; Meyer, T.; Veljković, D.Ž.; Medaković, V.B.; Knapp, E.-W.; Zarić, S.D. C–H/O interactions of aromatic CH donors within proteins: A crystallographic study. *Cryst. Growth Des.* **2016**, *16*, 1948–1957. [CrossRef]
45. Ji, W.; Liu, G.; Li, Z.; Feng, C. Influence of C–H···O hydrogen bonds on macroscopic properties of supramolecular assembly. *ACS Appl. Mater. Interfaces* **2016**, *8*, 5188–5195. [CrossRef] [PubMed]
46. Jones, C.R.; Baruah, P.K.; Thompson, A.L.; Scheiner, S.; Smith, M.D. Can a C–H···O interaction be a determinant of conformation? *J. Am. Chem. Soc.* **2012**, *134*, 12064–12071. [CrossRef] [PubMed]

47. Gu, Y.; Kar, T.; Scheiner, S. Fundamental properties of the C–H···O interaction: Is it a true hydrogen bond? *J. Am. Chem. Soc.* **1999**, *121*, 9411–9422. [CrossRef]
48. Jiang, L.; Lai, L. C–H···O hydrogen bonds at protein-protein interfaces. *J. Biol. Chem.* **2002**, *277*, 37732–37740. [CrossRef] [PubMed]
49. Scheiner, S. Dissection of the factors affecting formation of a C–H···O–H-bond. A Case Study. *Crystals* **2015**, *5*, 327–345. [CrossRef]
50. Desiraju, G.R.; Vittal, J.J.; Ramanan, A. *Crystal Engineering: A Textbook*; World Scientific: Singapore, 2011.
51. Babu, N.J.; Reddy, L.S.; Nangia, A. Amide*N*-oxide heterosynthon and amide dimer homosynthon in cocrystals of carboxamide drugs and pyridine *N*-oxides. *Mol. Pharm.* **2007**, *4*, 417–434. [CrossRef] [PubMed]
52. Goud, N.R.; Babu, N.J.; Nangia, A. Sulfonamide-pyridinen-*N*-oxide cocrystals. *Cryst. Growth Des.* **2011**, *11*, 1930–1939. [CrossRef]
53. Reddy, L.S.; Babu, N.J.; Nangia, A. Carboxamide-pyridine *N*-oxide heterosynthon for crystal engineering and pharmaceutical cocrystals. *Chem. Commun.* **2006**, 1369–1371. [CrossRef] [PubMed]
54. Puttreddy, R.; Cottam, J.R.A.; Steel, P.J. Anion dependent silver(I) complexes of pyrazine mono-*N*-oxide. *RSC Adv.* **2014**, *4*, 22449–22454. [CrossRef]
55. Rigaku Oxford Diffr. 2016; Version 1.171.38.41.
56. Bruker AXS BV. Madison, WI, USA, 1997–2004.
57. Otwinowski, Z.; Minor, W. Processing of X-ray diffraction data collected in oscillation mode. *Methods Enzymol.* **1997**, *276*, 307–326. [PubMed]
58. Blessing, R.H. Outlier treatment in data merging. *J. Appl. Crystallogr.* **1997**, *30*, 421–426. [CrossRef]
59. Sheldrick, G.M. Crystal structure refinement with SHELXL. *Acta Crystallogr. Sect. C* **2015**, *71*, 3–8. [CrossRef] [PubMed]
60. Dolomanov, O.V.; Bourhis, L.J.; Gildea, R.J.; Howard, J.A.K.; Puschmann, H. OLEX2: A complete structure solution, refinement and analysis program. *J. Appl. Crystallogr.* **2009**, *42*, 339–341. [CrossRef]
61. Farrugia, L.J. WinGX and ORTEP for Windows: An update. *J. Appl. Crystallogr.* **2012**, *45*, 849–854. [CrossRef]